

Stochastic fluctuation and transport in the edge tokamak plasmas with the resonant magnetic perturbation field

Minjun J. Choi,^{1, a)} Jae-Min Kwon,¹ Juhyung Kim,¹ Tongnyeol Rhee,¹ Jun-Gyo Bak,¹ Giwook Shin,¹ Hyun-Seok Kim,¹ Byoung-Ho Park,¹ Hogun Jhang,¹ Gunsu S. Yun,² Minwoo Kim,¹ Jong-Kyu Park,³ Hyung Ho Lee,¹ Yongkyoon In,⁴ Jaehyun Lee,¹ Min Ho Kim,² and Hyeon K. Park⁴

¹⁾*Korea Institute of Fusion Energy, Daejeon 34133, Republic of Korea*

²⁾*Pohang University of Science and Technology, Pohang, Gyungbuk 37673, Republic of Korea*

³⁾*Princeton Plasma Physics Laboratory, Princeton, New Jersey 08543, USA*

⁴⁾*Ulsan National Institute of Science and Technology, Ulsan 44919, Republic of Korea*

(Dated: 21 July 2022)

The stochastic layer formation by the penetration of the resonant magnetic perturbation (RMP) field has been considered as a key mechanism in the RMP control of the edge localized mode (ELM) in tokamak plasmas. Difficulty in measuring the stochasticity has limited the experimental identification of the narrow stochastic layer to ambiguous inference from the pressure profile change. Here, we suggest the rescaled complexity for an effective measure of the stochasticity to identify the stochastic layer in the plasma and also access the transport characteristics. We found that the fluctuation and transport in the edge plasmas become more stochastic with the more penetration of the RMP field into the plasma, which supports the importance of the stochastic layer formation in the RMP ELM control experiment.

^{a)}mjchoi@kfe.re.kr

INTRODUCTION

The edge localized mode (ELM) is a peeling-ballooning instability driven by the large current density and the steep pressure gradient in the high confinement mode (H-mode) pedestal in tokamak plasmas. Periodic collapses of the pedestal due to the explosive growth of the ELM have been a serious issue for steady-state operation of the H-mode plasmas. Applying the resonant magnetic perturbation (RMP) field is the most developed method to suppress the ELM and its pedestal collapse¹⁻⁶. Since the first demonstration of the RMP ELM suppression¹, many researches have followed for in-depth understanding of its mechanism. The initial idea of the stochastic edge transport⁷ was suggested¹, and later a narrow stochastic layer was considered promising to explain the experimental edge transport with the RMP field^{8,9}. It was more elaborated in the recent two-fluid MHD simulation that explained the ELM control process as sequential formation of narrow separated stochastic layers at the pedestal foot and top¹⁰. Resonant penetration of the perturbation field and consequent temperature flattening, supporting the stochastic layer formation inside the plasma, were observed in the experiment¹¹, but the lack of a proper measure of the stochasticity and the uncertainty in the profile diagnostics prohibit the further diagnosis and analysis which would be required for demonstration of the simulation results¹⁰. In this work, we suggest the rescaled Jensen Shannon complexity¹² for an effective measure of the stochasticity to identify the stochastic layer. We found that the stochasticity in electron temperature fluctuations is enhanced near the pedestal top in the RMP ELM suppression plasmas. The stochastic layer full width is estimated as 2.6 ± 2.0 cm localized at the pedestal top, where the two-dimensional electron cyclotron emission imaging diagnostics¹³ allowed the enhanced radial resolution of electron temperature measurements. Further analysis of the stochasticity in the particle flux around the striking point measured by the divertor Langmuir probe¹⁴ suggests the sequential enhancement of the stochasticity in the edge particle transport. Our results support the importance of the stochastic layer formation in the RMP ELM control and provide a method to identify the stochastic layer beyond the limitation of the profile diagnostics.

RESULTS

An example of the RMP ELM suppression in the KSTAR¹⁵ H-mode plasma #18945 is shown in Fig. 1. The $n = 1$ RMP field is applied from $t = 3.5$ sec and its strength increases in time. The line averaged plasma density (n_e) drops about 17 % with applying the RMP field while the edge electron temperature (T_e) drops about 9 %. This is the so-called density pump-out process. n_e and T_e are obtained by two color interferometry diagnostics¹⁶ and the electron cyclotron emission diagnostics¹⁷,

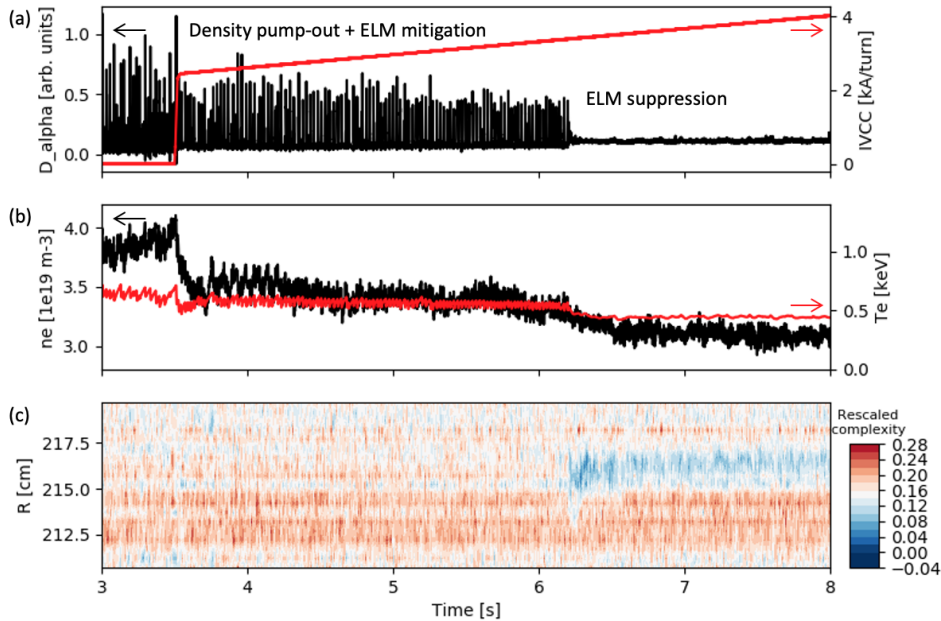


FIG. 1. (Color online) (a) The D_{α} emission (black) and the in-vessel coil current for the resonant magnetic perturbation (RMP) field (red). The edge localized mode (ELM) is suppressed with the increased RMP field. (b) The line averaged plasma density (n_e) and the edge electron temperature (T_e). (c) Spatiotemporal evolution of the rescaled Jensen Shannon complexity obtained by multiple T_e measurements in the pedestal region around the ELM location ($R_{\text{ELM}} = 215.2$ cm).

respectively. The ELM crash is mitigated with the RMP field and it is completely suppressed after $t \sim 6.2$ sec based on the D_{α} signal in Fig. 1(a) whose sharp rise indicates the ELM crash event. Modest decrease of n_e and the edge T_e during a transition from the ELM mitigation phase to the ELM suppression phase is observed, which indicates that the pedestal pressure height is reduced to make the ELM stable.

Formation of the stochastic layer in the pedestal region has been considered as a key mechanism of the RMP ELM suppression⁸⁻¹⁰. Although a direct measurement of fine structures of the magnetic field is not possible yet in tokamaks, local measurements of other plasma parameters in the pedestal region could be utilized to investigate the pedestal state for identification of the stochastic layer. In this work, local measurements of the low- k ($k\rho_i < 1$ where k is the wavenumber and ρ_i is the ion Larmor radius) T_e fluctuations from the electron cyclotron emission imaging (ECEI) diagnostics¹³ are used. In order to assess the degree of the stochasticity in the T_e fluctuations, the rescaled Jensen Shannon complexity is calculated.

The Jensen Shannon complexity ($C_{\text{JS}} = QH$)¹² is defined as the product of the normalized Shannon entropy $H = S/S_{\text{max}}$, where $S = S(P) = -\sum_i p_i \log(p_i)$ is the Shannon entropy of the given probability distribution function $P = \{p_i\}$ and S_{max} is the maximum entropy, and the Jensen

Shannon divergence $Q \propto S\left(\frac{P+P_e}{2}\right) - \frac{S(P)}{2} - \frac{S(P_e)}{2}$ where P_e is the uniform probability distribution function. It measures kind of the distance between the given probability distribution function and the uniform probability distribution function which would correspond to the most stochastic case. The $C_{\text{JS}}-H$ plane analysis based on the Bandt-Pompe (BP) probability distribution function¹⁸ is known as a useful method to quantify the stochasticity in the time series data^{12,19,20}. The signal can be called stochastic if its BP probability results in C_{JS} close to or smaller than C_{JS} of fractional Brownian motion (fBm) and fractional Gaussian noise (fGn) signals having the same H ¹². The BP probability represents the occurrence probability of an amplitude ordering of finite size (d) consecutive values with the same time step (Δt)¹⁸. For d consecutive values, there are $d!$ possible ways of the amplitude ordering, and the BP probability p_i means how frequently the i -th order-permutation appears in a time series data in total N points, i.e.

$$p_i = \frac{\text{the number of } d \text{ consecutive values whose amplitude order is represented by the } i^{\text{th}} \text{ permutation}}{\text{total number of } d \text{ consecutive values in available data}}$$

N should be large enough than $d!$ ($N \gg d!$) for the reliable calculation of the BP probability¹⁸.

The BP probability calculation parameters such as d , Δt , and N should be carefully determined for meaningful results. In this work, $d = 5$ and $\Delta t = 1$ us (for the Langmuir probe data, see below) or $\Delta t = 2$ us (for the ECEI data) are used so that $d\Delta t$ can be close to the time of interest. The time of interest in the ECEI data analysis is the transit time of pedestal structures over the ECEI channel measurement area where its size would be about 2 cm and the laboratory frame transit velocity is around 1–10 km/s. For the Langmuir probe data analysis, the time of interest is determined by considering the short pulses in the data²⁰. N is chosen as 5000 (for $\Delta t = 1$ us) or 2500 (for $\Delta t = 2$ us) which satisfies $N \gg d! = 120$ and provides the 5 ms time resolution of the calculation. A fast temporal resolution of the BP probability or C_{JS} calculation is required to study the prompt plasma response to the RMP field.

For the efficient comparison of C_{JS} to that of fBm or fGn signals, it is rescaled as

$$\hat{C} = \frac{C_{\text{JS}} - C_0}{|C_{\text{bdry}} - C_0|} \quad (1)$$

where $C_0(H)$ is the Jensen Shannon complexity of fBm or fGn signals and $C_{\text{bdry}}(H)$ is the maximum (if $C_{\text{JS}} > C_0$) or minimum (if $C_{\text{JS}} < C_0$) Jensen Shannon complexity at the given H . The rescaled complexity (\hat{C}) ranges from -1 ($C_{\text{JS}} = C_{\text{min}}$) to 1 ($C_{\text{JS}} = C_{\text{max}}$), and the less \hat{C} means the more stochastic.

The analysis result of the ECEI data shows that measured T_e fluctuations over the pedestal top region become more stochastic in the RMP ELM suppression phase. Spatiotemporal evolution of \hat{C} measurements using multiple ECEI channels in #18945 is shown in Fig. 1(c). Measurements from ECEI channels over (R, z) space are mapped into the radial coordinate on the z line of the

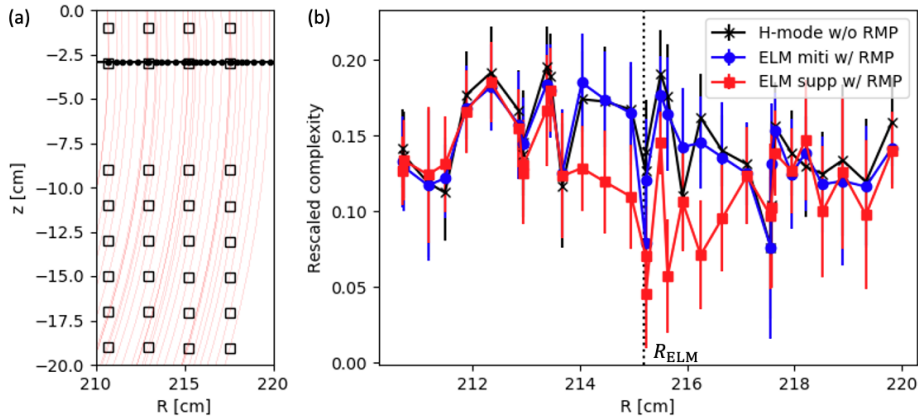


FIG. 2. (Color online) (a) The channel positions (squares) of the electron cyclotron emission imaging diagnostics used for calculation of the rescaled Jensen Shannon complexity. They are mapped into the radial coordinate (black circles) following the flux surfaces (red thin lines) on the black vertical line crossing the plasma center. (b) The radial profile of the time averaged rescaled complexity of electron temperature fluctuations in different phases. The pedestal top ($R = R_{\text{ELM}}$, the location of the edge localized mode) is indicated by black dashed line. Error bars indicate the standard deviation during the time average period.

vertical plasma center to enhance the radial resolution of the measurement (see Fig. 2(a)). Note that some channels whose noise contributions are exceptional and the data during the ELM crash period are excluded in the measurements. It drops significantly near the pedestal top ($R_{\text{ELM}} = 215.2$ cm where the ELMs were detected in T_e fluctuations) with a transition to the ELM suppression phase, and remains at a lower level for the entire ELM suppression phase. The stochastic layer by the RMP field penetration and the island overlapping has a stochastic magnetic geometry¹⁰. The T_e fluctuations measured by the channel going through the stochastic layer are expected to be more stochastic, while the coherent fluctuations over regular magnetic geometry produced particular patterns which increase the rescaled complexity. Therefore, the lowered \hat{C} (enhanced stochasticity) of T_e fluctuations near the pedestal top suggests that the stochastic layer forms at the pedestal top and it plays an important role in the transition and maintenance of the ELM suppression.

The time averaged profile of \hat{C} shown in Fig. 2(b) provides an estimate of the stochastic layer full width. By the stochastic layer, we mean the region of the reduced \hat{C} compared to that of the inter ELM periods. Since each channel has different noise contribution, the relative change of \hat{C} profile among different averaging periods should be more meaningful than the absolute value of \hat{C} . The averaged \hat{C} profile is nearly same between the inter ELM periods of the H-mode w/o the RMP phase (black crosses) and the ELM mitigation w/ the RMP phase (blue circles). A significant drop of \hat{C} compared to other periods is observed locally near the pedestal top ($R = R_{\text{ELM}}$) in the ELM suppression period w/ the RMP phase (red squares). The full width of the enhanced stochasticity

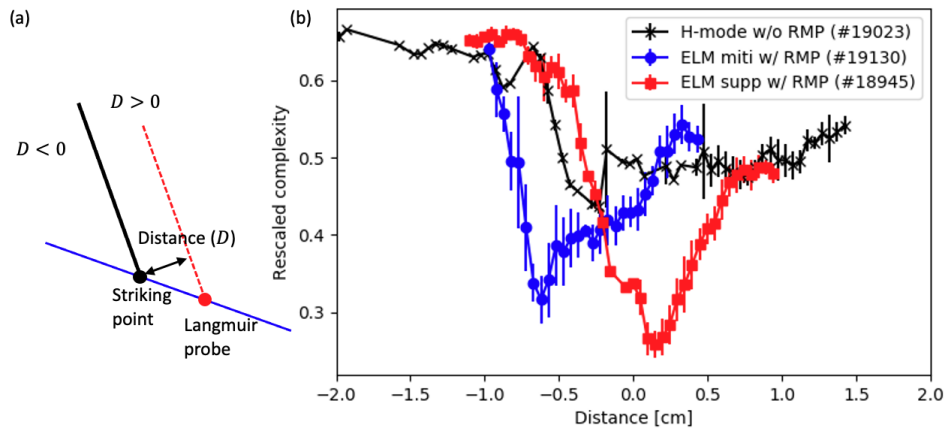


FIG. 3. (Color online) (a) The illustration for the distance (D) measurement between the flux surfaces of the striking point (black dot) and the Langmuir probe (red dot). D can have about 1 cm absolute error. The particle flux measurements along D are obtained as the striking point moves across the Langmuir probe with the plasma movement. (b) The radial profile of the rescaled complexity of the particle flux around the striking point in different phases. The same Langmuir probe is used for direct comparison of the profiles from different plasmas. Error bars indicate the standard deviation of the measurements.

region can be estimated as the range of the \hat{C} reduction more than the standard deviation of \hat{C} measurements, which is about 2.6 ± 2.0 cm considering the finite size (~ 2 cm) of measurement area of each ECEI channel. The flux surface distortion by the field penetration which caused the overestimation of the stochastic layer full width should be taken into account for a more accurate estimation.

It would be interesting to compare this experimental observation with the result of the recent two-fluid numerical simulation¹⁰. The simulation suggested that a sequential formation of the stochastic layers at the pedestal foot and top could explain the density pump-out and the ELM suppression, respectively. The reduced \hat{C} (enhanced stochasticity) of the pedestal top T_e fluctuations in the ELM suppression phase of the KSTAR experiment can be consistent with the simulation result, but no evidence for multiple separated layers (reduced \hat{C} regions) is found. However, the ECE measurement in the pedestal foot region is uncertain due to the limited diagnostics capability with the low density and temperature of that region. For the quantitative comparison of the stochastic layer width, a sophisticated cross validation analysis matching all the important parameters such as the plasma resistivity would be necessary. A relatively large uncertainty in the stochastic layer width measurement due to the finite channel size suggests that the growing tendency of the width with the resistivity rather than the absolute value would be more feasible to be confirmed in the experiment, which is left for the future work.

Although a reliable analysis based on local measurements of the pedestal foot region was not

available, the Langmuir probe data which measures the ion saturation current ($I_{\text{sat}} \propto$ the particle flux) could be used to investigate any change of stochasticity in the particle transport in the far edge region with the RMP field. Measurements of the particle flux around the striking point are obtained by the divertor Langmuir probe when the striking point drifts across the probe location from three different plasmas for different phases, i.e. #19023 (H-mode w/o the RMP), #19130 (ELM mitigation w/ the RMP), and #18945 (ELM suppression w/ the RMP). Since the Langmuir probe data are not a local measurement of the pedestal region and taken from plasmas with different pedestal parameters such as q_{95} and RMP configurations, we should assume that the stochasticity of particle flux measured by the Langmuir probe can reflect the stochasticity of the particle transport in the pedestal region, or the degree of the field penetration, regardless of local pedestal parameters. Nonetheless, all the data could be obtained by one probe in the near term so that the absolute value of the rescaled complexity from different plasmas can be directly compared assuming the similar noise contribution. In fact, the base level of \hat{C} measurements in different plasmas has shown a similar value. \hat{C} measurements in time as the striking point moves across the probe location are transformed into \hat{C} measurements along the distance (D). This distance is defined as a distance between two flux surfaces containing the striking point and the probe as illustrated in Fig. 3(a). Equilibrium flux surfaces are reconstructed using EFIT code²¹ with the magnetic data, and D measurements can involve about 1 cm absolute error especially when the RMP field is applied. By the definition, $D = 0$ would correspond to the striking point, $D < 0$ to the private zone, and $D > 0$ to the typical scrape-off-layer region, respectively.

The \hat{C} profiles over the distance in Fig. 3(b) show that the edge particle transport across the separatrix becomes more stochastic with the RMP field. The \hat{C} profiles from different plasmas have a similar shape, i.e. it drops fast from $D \ll 0$ towards $D = 0$ and increases slowly over the $D > 0$ region. The fast drop would correspond to a transition from the private zone (where \hat{C} values of all plasmas are around the similar noise level) to the striking point. Interestingly, the minimum of \hat{C} which is expected to reside close to the striking point is found to be significantly different in different plasma conditions. It is lower in the ELM mitigation phase than in the H-mode phase, and the lowest value was found in the ELM suppression phase. This means that the particle flux becomes more and more stochastic as the plasma state changes from the H-mode to the ELM mitigation and from the ELM mitigation to the ELM suppression, which can result from the more RMP field penetrations as observed in the previous numerical simulation¹⁰.

Next, another interesting observation has been made using the pedestal top T_e fluctuations in the RMP ELM suppression experiment #18945. Fig. 4 shows the rescaled complexity and the total (squared) bicoherence in time using the T_e measurements from one ECEI channel close to the

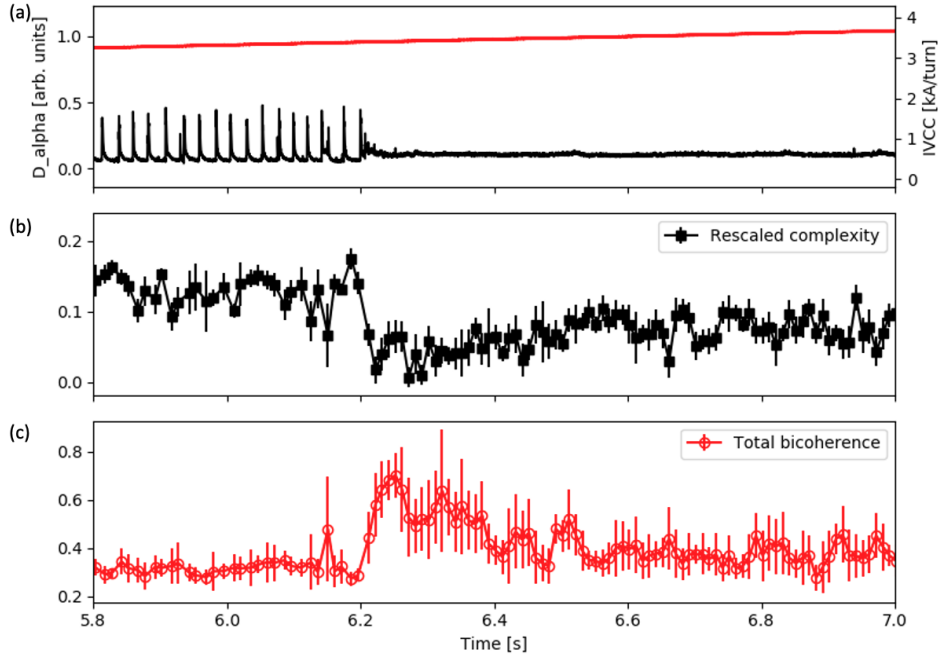


FIG. 4. (Color online) (a) The D_{α} emission (black) and the in-vessel coil current for the resonant magnetic perturbation (RMP) field (red). (b) The rescaled complexity and (c) the total bicoherence of the electron temperature fluctuation at the pedestal top (the edge localized mode location). Error bars indicate the standard deviation of the measurements.

pedestal top ($R = R_{\text{ELM}}$). The bicoherence calculations with the fast temporal resolution (milliseconds scale) were possible utilizing the Morlet wavelet transformation^{22,23} instead of the conventional Fourier transformation, and it is summed over 10–100 kHz range to identify the nonlinear three-wave coupling among the fluctuations.

A strong anti-correlation between \hat{C} and the total bicoherence was observed during the RMP ELM suppression phase. The total bicoherence at the pedestal top before the ELM suppression is around the noise level, and it rapidly increases²⁴ with the reduction of \hat{C} in a transition to the ELM suppression phase as shown in Fig. 4. Note that the T_e fluctuations in the H-mode without the RMP field do not exhibit any significant bicoherence or the correlated change of the rescaled complexity. The significant bicoherence means that the low- k T_e fluctuations measured by the ECEI diagnostics have the strong three-wave coupling which could be a passage for the fluctuation energy transfer. The synchronized change of the bicoherence and the rescaled complexity implies that the coupling among the fluctuations is via a small island of the narrow stochastic layer at the pedestal top. The resonant behavior between turbulence and an island of the comparable size, which is reported in reference²⁵, could be responsible for the appearance of the significant bicoherence with the field penetration. Recently, the interaction between an island and small scale fluctuations has been extensively studied^{26,27}. Their interactions can result in the coupled

evolution^{23,28}. Understanding the formation and evolution of the stochastic layer in the pedestal region should also require considering intricate multi-mode coupling effects.

SUMMARY

In summary, we found that the rescaled complexity can be utilized to identify the stochastic layer in the plasma and access the transport characteristics. Both the electron temperature fluctuations and the particle flux become more stochastic as the RMP field penetrates into the edge plasma. This observation is not inconsistent with the expected formation of the stochastic layer through which the fluctuation and transport would have the stochastic behavior. The formation and evolution of the stochastic layer can involve the complex dynamics such as the nonlinear interaction among small scale modes which would affect the transport in the pedestal region.

ACKNOWLEDGMENTS

This research was supported by R&D Programs of “KSTAR Experimental Collaboration and Fusion Plasma Research(EN2101-12)” and “High Performance Fusion Simulation R&D(EN2141-7)” through Korea Institute of Fusion Energy (KFE) funded by the Government funds and by National Research Foundation of Korea under NRF-2019M1A7A1A03088462.

REFERENCES

- ¹T. E. Evans, R. A. Moyer, P. R. Thomas, J. G. Watkins, T. H. Osborne, J. a. Boedo, E. J. Doyle, M. E. Fenstermacher, K. H. Finken, R. J. Groebner, M. Groth, J. H. Harris, R. J. La Haye, C. J. Lasnier, S. Masuzaki, N. Ohyabu, D. G. Pretty, T. L. Rhodes, H. Reimerdes, D. L. Rudakov, M. J. Schaffer, G. Wang, and L. Zeng, *Physical Review Letters* **92**, 235003 (2004).
- ²Y. Liang, H. Koslowski, P. Thomas, E. Nardon, B. Alper, P. Andrew, Y. Andrew, G. Arnoux, Y. Baranov, M. Becoulet, M. Beurskens, T. Biewer, M. Bigi, K. Crombe, E. de la Luna, P. de Vries, W. Fundamenski, S. Gerasimov, C. Giroud, M. Gryaznevich, N. Hawkes, S. Hotchin, D. Howell, S. Jachmich, V. Kiptily, L. Moreira, V. Parail, S. Pinches, E. Rachlew, and O. Zimmermann, *Physical Review Letters* **98**, 265004 (2007).
- ³Y. M. Jeon, J. K. Park, S. W. Yoon, W. H. Ko, S. G. Lee, K. D. Lee, G. S. Yun, Y. U. Nam, W. C. Kim, J.-G. Kwak, K. S. Lee, H. K. Kim, and H. L. Yang, *Physical Review Letters* **109**, 035004 (2012).

- ⁴Y. Sun, Y. Liang, Y. Q. Liu, S. Gu, X. Yang, W. Guo, T. Shi, M. Jia, L. Wang, B. Lyu, C. Zhou, A. Liu, Q. Zang, H. Liu, N. Chu, H. H. Wang, T. Zhang, J. Qian, L. Xu, K. He, D. Chen, B. Shen, X. Gong, X. Ji, S. Wang, M. Qi, Y. Song, Q. Yuan, Z. Sheng, G. Gao, P. Fu, and B. Wan, *Physical Review Letters* **117**, 115001 (2016).
- ⁵W. Suttrop, A. Kirk, R. Nazikian, N. Leuthold, E. Strumberger, M. Willensdorfer, M. Cavedon, M. Dunne, R. Fischer, S. Fietz, J. C. Fuchs, Y. Q. Liu, R. M. McDermott, F. Orain, D. A. Ryan, E. Viezzer, the ASDEX Upgrade Team, The DIII-D Team, and the EUROfusion MST1 Team, *Plasma Physics and Controlled Fusion* **59**, 014049 (2016).
- ⁶J. K. Park, Y. Jeon, Y. In, J.-W. Ahn, R. Nazikian, G. Park, J. Kim, H. Lee, W. Ko, H.-S. Kim, N. C. Logan, Z. Wang, E. A. Feibush, J. E. Menard, and M. C. Zarnstropp, *Nature Physics* **14**, 1223 (2018).
- ⁷A. B. Rechester and M. N. Rosenbluth, *Physical Review Letters* **40**, 38 (1978).
- ⁸G. Park, C. S. Chang, I. Joseph, and R. A. Moyer, *Physics of Plasmas* **17**, 102503 (2010).
- ⁹P. B. Snyder, T. H. Osborne, K. H. Burrell, R. J. Groebner, A. W. Leonard, R. Nazikian, D. M. Orlov, O. Schmitz, M. R. Wade, and H. R. Wilson, *Physics of Plasmas* **19**, 056115 (2012).
- ¹⁰Q. M. Hu, R. Nazikian, B. A. Grierson, N. C. Logan, C. Paz-Soldan, and Q. Yu, *Nuclear Fusion* **60**, 076001 (2020).
- ¹¹R. Nazikian, C. Paz-Soldan, J. D. Callen, J. S. DeGrassie, D. Eldon, T. E. Evans, N. M. Ferraro, B. A. Grierson, R. J. Groebner, S. R. Haskey, C. C. Hegna, J. D. King, N. C. Logan, G. R. McKee, R. A. Moyer, M. Okabayashi, D. M. Orlov, T. H. Osborne, J. K. Park, T. L. Rhodes, M. W. Shafer, P. B. Snyder, W. M. Solomon, E. J. Strait, and M. R. Wade, *Physical Review Letters* **114**, 105002 (2015).
- ¹²O. A. Rosso, H. A. Larrondo, M. T. Martin, A. Plastino, and M. A. Fuentes, *Physical Review Letters* **99**, 154102 (2007).
- ¹³G. S. Yun, W. Lee, M. J. Choi, J. Lee, M. Kim, J. Leem, Y. Nam, G. H. Choe, H. K. Park, H. Park, D. S. Woo, K. W. Kim, C. W. Domier, N. C. Luhmann, N. Ito, A. Mase, and S. G. Lee, *Review of Scientific Instruments* **85**, 11D820 (2014).
- ¹⁴J. G. Bak, H. S. Kim, M. K. Bae, J. W. Juhn, D. C. Seo, E. N. Bang, S. B. Shim, K. S. Chung, H. J. Lee, and S. H. Hong, *Journal of Nuclear Materials* **463**, 424 (2015).
- ¹⁵H. K. Park, M. J. Choi, S. H. Hong, Y. In, Y. M. Jeon, J. S. Ko, W. H. Ko, J. G. Kwak, J. M. Kwon, J. Lee, J. H. Lee, W. Lee, Y. B. Nam, Y. K. Oh, B. H. Park, J. K. Park, Y. S. Park, S. J. Wang, M. Yoo, S. W. Yoon, J. G. Bak, C. S. Chang, W. H. Choe, Y. Chu, J. Chung, N. Eidietis, H. S. Han, S. H. Hahn, H. G. Jhang, J. W. Juhn, J. H. Kim, K. Kim, A. Loarte, H. H. Lee, K. C. Lee, D. Mueller, Y. S. Na, Y. U. Nam, G. Y. Park, K. R. Park, R. A. Pitts, S. A. Sabbagh, G. S.

- Yun, and the KSTAR team, *Nuclear Fusion* **59**, 112020 (2019).
- ¹⁶K. C. Lee, J. W. Juhn, Y. U. Nam, Y. S. Kim, H. M. Wi, S. W. Kim, and Y. c. Ghim, *Fusion Engineering and Design* **113**, 87 (2016).
- ¹⁷S. H. Jeong, K. D. Lee, Y. Kogi, K. Kawahata, Y. Nagayama, A. Mase, and M. Kwon, *Review of Scientific Instruments* **81**, 10D922 (2010).
- ¹⁸C. Bandt and B. Pompe, *Physical Review Letters* **88**, 174102 (2002).
- ¹⁹J. E. Maggs, T. L. Rhodes, and G. J. Morales, *Plasma Physics and Controlled Fusion* **57**, 045004 (2015).
- ²⁰Z. Zhu, A. E. White, T. A. Carter, S. G. Baek, and J. L. Terry, *Physics of Plasmas* **24**, 042301 (2017).
- ²¹L. L. Lao, H. S. John, R. D. Stambaugh, A. G. Kellman, and W. Pfeiffer, *Nuclear Fusion* **25**, 1611 (1985).
- ²²B. P. van Milligen, E. Sánchez, T. Estrada, C. Hidalgo, B. Brañas, B. Carreras, and L. García, *Physics of Plasmas* **2**, 3017 (1995).
- ²³M. J. Choi, L. Bardóczi, J.-M. Kwon, T. S. Hahm, H. K. Park, J. Kim, M. Woo, B.-H. Park, G. S. Yun, E. Yoon, and G. McKee, *Nature Communications* **12**, 375 (2021).
- ²⁴J. Lee, G. S. Yun, M. J. Choi, J.-M. Kwon, Y.-M. Jeon, W. Lee, N. C. Luhmann, and H. K. Park, *Physical Review Letters* **117**, 075001 (2016).
- ²⁵F. L. Waelbroeck, J. W. Connor, and H. R. Wilson, *Physical Review Letters* **87**, 215003 (2001).
- ²⁶A. Ishizawa, Y. Kishimoto, and Y. Nakamura, *Plasma Physics and Controlled Fusion* **61**, 054006 (2019).
- ²⁷K. Ida, *Plasma Physics and Controlled Fusion* **62**, 014008 (2020).
- ²⁸W. Chen, M. Jiang, Y. Xu, P. W. Shi, L. M. Yu, X. T. Ding, Z. B. Shi, X. Q. Ji, D. L. Yu, Y. G. Li, Z. C. Yang, W. L. Zhong, Z. Y. Qiu, J. Q. Li, J. Q. Dong, Q. W. Yang, Y. Liu, L. W. Yan, M. Xu, and X. R. Duan, *Nuclear Fusion* **57**, 114003 (2017).